Experimental Method to Find the Optimum Excitation Waveform to Quench Mechanical Resonances of Fabry–Pérot Tunable Filters Used in Swept Sources

I. Trifanov, A. Bradu, L. Neagu, P. Guerreiro, A. B. Lobo Ribeiro, and A. Gh. Podoleanu

***Abstract*—We report experimental evidence of improving the nonlinearity of conventional wavelength swept laser sources based on a fiber Fabry–Pérot tunable filter as a wavelength-selective element. Our solution is based on applying a nonsinusoidal, synthesized waveform to the tunable filter that can be identified experimentally. A significant improvement in the optical coherence tomography image quality has been obtained without any software recalibration method.**

***Index Terms*—Fabry–Pérot tunable filter (FP-TF), optical coherence tomography (OCT), swept source (SS).**

I. Introduction

MOST wavelength swept laser sources (SS) that use a scanning Fabry–Pérot tunable filter (FP-TF) exhibit a nonlinear temporal change of frequency due to the typical sinusoidal excitation waveform applied to the piezoelectric (PZT) element controlling the filter. Ideally, a linear arrangement of data along the k-axis (in wavenumber) is required prior to Fast Fourier Transformation (FFT) in order to yield a correct depth profile. Incorrect optical frequency mapping leads to an A-scan with broadened peaks, that exhibits distortions similar to those due to dispersion left uncompensated in the interferometer. To compensate for the source nonlinearities, three solutions have been proposed: (i) using a software approach, consisting in resampling the data after analogue-to-digital conversion (A/D) [1]; (ii) using a hardware approach, consisting in clocking the A/D with an electronic trigger-signal (K-trigger) generated by a second interferometer [2] and (iii) driving the FP-TF with a superposition of sinusoidal waveforms at the first three harmonics of the filter resonance frequencies [3]. These solutions have their own limitations, (i) is computationally intensive and reduces the frame rate; (ii) is characterized by a higher cost due to the need of a second interferometer and special hardware, including that of a fast digitizer equipped with a specialized clock required to work within a large range of frequencies; (iii) requires a complex numerical iterative optimization algorithm with 7 variables (amplitudes and phases of the three harmonics and the center wavelength offset) based on a predefined parameter and error maps, and fine experimental adjustments are still needed for final optimization.

Manuscript received December 23, 2010; revised February 28, 2011; accepted March 26, 2011. Date of publication April 07, 2011; date of current version May 25, 2011. This work was supported in part by the European project HIRESOMI (Marie Curie EC MEST-CT-2005-020353). The work of A. Bradu and A. G. Podoleanu was supported by the European Research Council under Grant 249889.

I. Trifanov and P. Guerreiro are with Multiwave Photonics S.A., 4470-605 Moreira da Maia, Portugal (e-mail: itrifanov@multiwavephotonics.com; pguerreiro@multiwavephotonics.com).

A. Bradu, L. Neagu, and A. G. Podoleanu are with the Applied Optics Group, School of Physical Sciences, University of Kent, Canterbury, Kent CT2 7NR, U.K. (e-mail: A.Bradu@kent.ac.uk; liviu.neagu@gmail.com; A.G.H.Podoleanu@kent.ac.uk).

A. B. Lobo Ribeiro is with the Faculty of Health Sciences, University Fernando Pessoa, 4200-150 Porto, Portugal (e-mail: alobo@ufp.edu.pt).

Digital Object Identifier 10.1109/LPT.2011.2140101

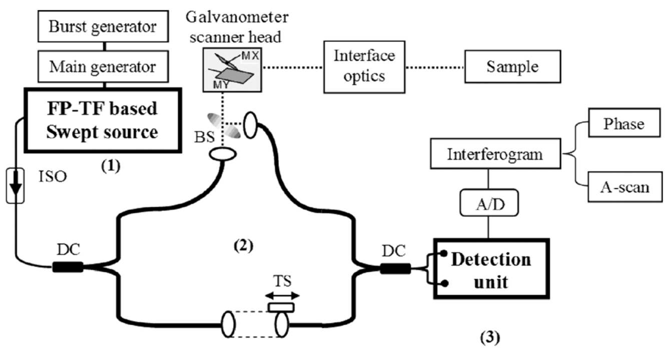

Fig. 1. Schematic diagram of the SS-OCT configuration. It consists of (1) a FP-TF-based swept laser source, (2) an OCT interferometer, and (3) a balanced photodetection unit. Two frequency generators (main and burst generators) are employed for iterative control of the FP-TF.

In this letter, we propose a different hardware approach based on generating a synthesized anti-phase modulation waveform function that is applied to the FP-TF. The waveform is found experimentally during an iterative hardware adjustment process. The optimization is simple and rapid, seeking minimum width of the FFT peak for a given optical path difference (OPD) value in the OCT interferometer, where the object is replaced with a mirror. Our solution does not require a separate characterization setup, as used by method (iii).

II. Experimental Configuration

The swept-source OCT (SS-OCT) configuration is depicted in Fig. 1. The swept laser source [4], [5] is configured as an optical resonator that includes a semiconductor optical amplifier (SOA) as a fast dynamic gain medium (1060 nm, Superlum) and a high-speed piezoelectrically driven tuning wavelength element (FP-TF, LambdaQuest). The filter operates at 1060 nm central wavelength, with a free spectral range of ~75 nm, 0.12 nm linewidth, up to 40 kHz tuning frequency and an insertion loss of 2.5 dB. A proper optical isolation (ISO) is required before coupling to an external device.

To study the linearity in k-space of such a source, its output is coupled to an OCT system designed as a Mach–Zehnder fiber interferometer constructed with two directional couplers (DC). Part of the light is sent via a bulk beamsplitter (BS) to the sample arm comprising of a pair of orthogonal galvo-scanners and interface optics for 3-D biological tissue imaging. The backscattered signal from the sample is coherently recombined with the reference arm at the detector and the OPD is adjusted using a translation stage (TS). The interference signal is detected using a homemade balanced P-i-N photodiode detection block (4 MHz bandwidth), with internal adjustable gain and adjustable balance of photodetecting signals. Data acquisition was performed using a high speed A/D card operating at 200 MSamples/s with 12-bit resolution (National Instruments, model NI 5124). The card is controlled by a LabView software program that performs the FFT and displays the interferogram in real time. Both the amplitude of the A-scan as well as the phase variation along the scanned channelled spectrum are displayed.

III. Method

For a linear excitation of the tunable filter using a ramp or a sawtooth at slow speed (around 1 kHz), the wavelength generated, λ, varies linearly in time. In such a regime, simple software linearization to convert the data to exhibit linear dependence to optical frequency, ν ($\nu = c/\lambda$, where c is the speed of light), can provide correct A-scan profiles. However, when increasing the excitation frequency, the shorter time required for changing the slope of variation from one ramp to the next becomes closer to the inverse of the mechanical resonance of the FP-TF. Consequently, the higher the frequencies of the applied signal the larger the deviation of the mechanical response of the FP-TF from the applied drive waveform. This determines a profound nonlinear frequency response of the filter that renders the software linearization inefficient. This phenomenon limits the maximum frequency of the signal applied to the FP-TF.

The nonlinear response of the filter, although linearly excited at 5 kHz with a ramp waveform, is clearly visible as shown in Fig. 2 (top row). The modulation of the phase of the interferogram (top middle) is the response of this filter to different harmonics of the sawtooth applied. Also, the FFT of the interferogram (top right) shows broadening of the signal coming from a plane reflector.

Our method consists in adding a second waveform (Burst generator) to the linear ramp (Main generator). By varying the frequency of the second waveform, we realized that we could excite the resonances of the FP-TF and make the phase even more nonlinear. This suggests that if similar excitation is applied, but in antiphase, it may reduce the mechanical resonances of the filter and its nonlinearity behavior. The proposed hardware solution is illustrated schematically in Fig. 3. The waveform at the top in Fig. 3 shows the main excitation which determines the operation conditions of the source in terms of frequency sweep, tuning range and duty cycle. The amplitude and the bias voltage of the 1st waveform applied determine the tuning bandwidth (typically 40 nm in this experiment) and the center wavelength (~1060 nm), respectively. Usually, the bias is adjusted to overlap the tuning frequency range of the filter with that of the gain medium. The frequency of the

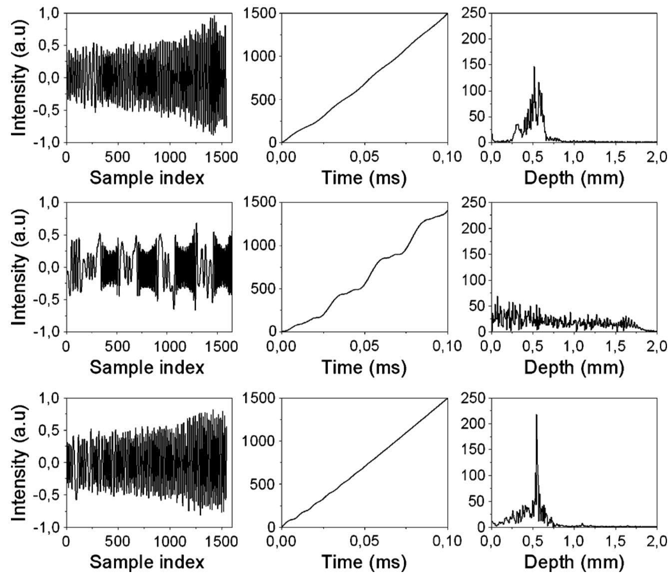

Fig. 2. Interferogram (left), phase (middle), and FFT transform (right) obtained from a mirror object placed in the sample arm of the SS-OCT setup. The results were obtained by using: linear excitation at 5 kHz only (top row); modulation at 50 kHz close to the first resonance of the FP-TF in addition to the linear excitation (middle row); the optimized synthesized shape: four burst pulses of sine wave at 101-kHz frequency, with 0.5-V_{PP} amplitude and 28° phase superimposed to the linear excitation at 5 kHz (bottom row).

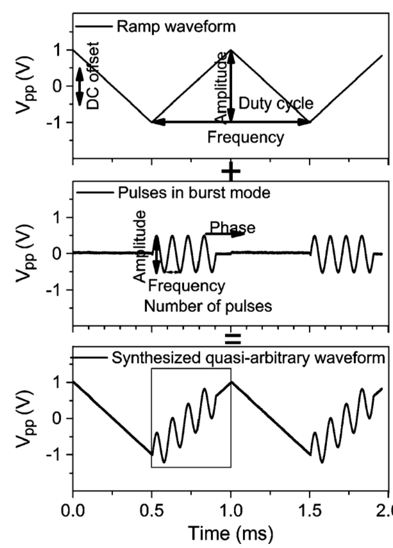

Fig. 3. Signal applied to the FP-TF. Top: first waveform, linear excitation. Middle: second waveform, burst pulses consisting of four sinusoidal cycles. Bottom: synthesized waveform obtained by adding the waveforms above with an adjustable phase difference in between.

main waveform gives the frequency sweep of the source or the A-scan acquisition speed of the OCT system. In the example shown in Fig. 2, this was set at 5 kHz with a duty cycle of 50% (triangular waveform). The chosen sweep duration equals half of the cycle duration which in principle can be doubled to a 10 kHz effective sweep frequency in a 2× buffering scheme.

To correct for the nonlinearities of the filter response, a second waveform was applied. This consists in a sequence of pulses in burst mode, generated by a Stanford Research function generator (model DS345). This can be used to generate a number of complete waveform cycles, for each trigger applied, as displayed in Fig. 3 (middle). Burst mode may be used with any arbitrary waveform at any frequency. Full control over the number of pulses, frequency, amplitude and phase is available. The generator is equipped with phase control that allows altering the time of the burst relative to the main waveform by using a trigger synchronized with the main generator. Delay by up to one-half of a period of the burst frequency with respect to an external trigger is possible. The resulting waveform applied to the FP-TF is a quasi-arbitrarily synthesized waveform as displayed in Fig. 3 (bottom). This illustrates an example of the shape of the waveform applied to the FP-TF.

By changing the frequency of the modulation applied from the burst generator in steps of 2 kHz at low amplitude (0.5 V and 0 phase), we have been able to identify visually from the interferogram and quantitatively from phase information, FP-TF resonances at approximately 50 kHz, and 100 kHz. Fig. 2 (middle row) displays the response of the filter at the first resonance. Near a resonance, the nonlinearity is exacerbated. This results in an interferogram exhibiting high nonuniformity in fringe spacing (middle row, left), which translates in a high modulation of the phase (middle row, middle) and excessive broadening of the FFT (middle row, right). However, shifting the pulses in time, that is, iteratively increasing the phase values, allows for partially counteracting the effect of the modulation induced by the filter.

IV. Results

In practice, the parameters of amplitude and phase of the bursts are altered iteratively in order to find the best match that corrects for the nonlinearities of the filter. These are performed while keeping the sinusoidal frequency of the second waveform fixed, close to the first, second or the third resonances of the FP-TF. The adjustment depended critically on the phase and frequency of the bursts and less on the number of cycles in the bursts. Fewer cycles could be compensated with larger amplitudes to achieve similar effects. However, excessive amplitude applied should be avoided especially when driving the filter near its resonances, because of the electromechanical load that may cause overheating and damage.

Fig. 2 (bottom row) shows the results obtained when the optimum quasi-arbitrarily synthesized waveform is applied. A significant improvement is achieved in terms of the width and shape of the A-scan. The optimum parameters found for correcting the response of the filter when using a linear excitation at 5 kHz (triangular waveform) and 8 V amplitude were: 4 burst pulses of sine waves at 101 kHz frequency, with 0.5 V_{pp} amplitude and 28 degree phase. If the sine wave frequency deviated from 101 kHz by more than 5 kHz either side, no correction was obtained, even if other phase values were tested.

A set of B-scan OCT images from a sample made of 13 layers of cello tape of 78 μm thickness (measured in air) is displayed in Fig. 4 to illustrate the efficiency of the method. Lateral scanning was performed by applying 3.5 V to one of the transversal scanners in the OCT sample arm at a frame rate of 11.4 Hz. Fig. 4 left displays considerable distortions in the OCT image caused by nonlinear tuning, when the main excitation at 5 kHz was applied alone. The image in the right shows the result after optimization of the waveform using the parameters mentioned in the text. No calibration step or spectral apodization prior to FFT was performed in either case. The image was presented with no software linearization to prove that the technique can significantly contribute towards quenching the resonances of the filter.

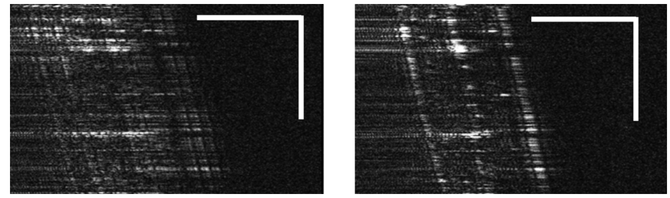

Fig. 4. B-scan OCT images obtained using a linear excitation (left) and the optimum synthesized shape (right). Scale bars represent 1 mm.

V. Conclusion

The technique presented here can be employed in practice as a simple, low cost solution for compensating for nonlinear response of the FP-TF used in swept sources. The technique was demonstrated experimentally for a FP-TF based SS where the initial maximum frequency sweep was less than 5 kHz. The technique proposed consists in experimental identification of a synthesized waveform, consisting in superposition of a main linear waveform with sinusoidal bursts. The number of parameters that need to be identified is 3 only (frequency of the sinusoidal signal in the burst, its amplitude and phase in relation to the main waveform) without any need for computational calculations. The range of burst frequencies needed can be easily identified by first exacerbating the nonlinear effect that can be easily followed using the digital processing electronic interface which equips any SS-OCT system. This provides the distortion of phase curve and of the FFT peaks that could be used to guide the search for optimum parameters.

References

[1] S. Vergnole, D. Lévesque, and G. Lamouche, "Experimental validation of an optimized signal processing method to handle non-linearity in swept-source optical coherence tomography," *Opt. Express*, vol. 18, pp. 10446–10461, 2010.

[2] J. Xi, L. Huo, J. Li, and X. Li, "Generic real-time uniform K-space sampling method for high-speed swept-Source optical coherence tomography," *Opt. Express*, vol. 18, pp. 9511–9517, 2010.

[3] C. M. Eigenwillig, B. R. Biedermann, G. Palte, and R. Huber, "K-space linear Fourier domain mode locked laser and applications for optical coherence tomography," *Opt. Express*, vol. 16, pp. 8916–8937, 2008.

[4] I. Trifanov, L. Neagu, A. Bradu, A. G. Podoleanu, and A. B. Lobo Ribeiro, "Characterization of a swept source at 1 μm for optical coherence tomography," *Proc. SPIE*, vol. 7889, 2011, Paper 7889-100.

[5] R. Huber, M. Wojtkowski, K. Taira, J. Fujimoto, and K. Hsu, "Amplified, frequency swept lasers for frequency domain reflectometry and OCT imaging: Design and scaling principles," *Opt. Express*, vol. 13, pp. 3513–3528, 2005.